Electronic Supplementary Material (ESI) for New Journal of Chemistry.

SUPPORTING INFORMATION

A unique dual sensor for the detection of DCNP (nerve agent mimic) and Cd^{2+} in water

Ayndrila Ghosh,[†] Sujoy Das,[†] Saurodeep Mandal and Prithidipa Sahoo*

[†]Equal contribution to the work.

Department of Chemistry, Siksha Bhavana (Institute of Science), Visva-Bharati, Santiniketan, 731235, W.B., India.

.

Table S1. Performance Comparison of Existing Methods and Present Methods based on chemosensors for Determination of DCNP (a Tabun mimic).

Analytes	Sensor type	Detection limit(nM)	Detection medium	Detection method	Detection state	Sensitivity & Selectivity	Response Time	Estimation in samples	Reference
DCNP (Tabun mimic)	**Carbazole**	**7.75**	**Neutral**	**Naked eye UV-Vis**	**Liquid Gas**	**High**	**Real time**	**Water**	**Current method**
Tabun	Trifluoromethylphenyl	0.05-1.0 mg	nd	Naked eye UV-Vis	Liquid	High	Real time	nd	Analyst. 2011, 136, 5151-5156.
DCNP, DCP	N,N-dimethylaniline	nd	Neutral	Naked eye UV-Vis	Liquid	High	Few minutes	nd	Chem. Eur. J. 2011, 17, 6931-6934
DMMPDCP DCNP	Zn(II)-bis-terpyridine systems	1-10	nd	Fluorescence	Liquid, Gas	High	10 min	nd	Chem. Commun., 2012, 48, 964-966.
DECP (DCNP)	BODIPY-salicylaldehydeoxime conjugation	922	Neutral	Fluorescence	Liquid	High	nd	nd	Chem. Commun., 2014, 50, 7531-7534.
DCNP	BODIPY	1-10	Neutral	Fluorescence	Liquid	Moderate	45-90 min	nd	Chem. Commun., 2012, 48, 4767–4769.
DCNP DFP	Aryl carbinol	5×10^2-16×10^2	nd	Naked eye, UV-vis	Liquid	Moderate	5 min	nd	New J. Chem., 2012, 36, 1485–1489
DCP, DCNP, DFP	BODIPY	nd	nd	Fluorescence	Liquid, Gas	Moderate	10-20 seconds	nd	Chem. Eur. J. 2016, 22, 1 – 6

DCNP, DFP	Tert-butyldimethylsilylether (TBDMS)	200	Neutral	Naked eye, UV-vis	Liquid, Gas	High	30 seconds	nd	Chem. Eur. J. 2011, 17, 11994 – 11997
DCNP, DFP	Tryarylmethanol	300	Neutral	Naked eye, UV-vis	Liquid, Gas	High	5-10 min	nd	Eur. J. Org. Chem. 2012, 4937–4946

1. NMR Studies:

^{1}H NMR of CPC in DMSO-d_6:

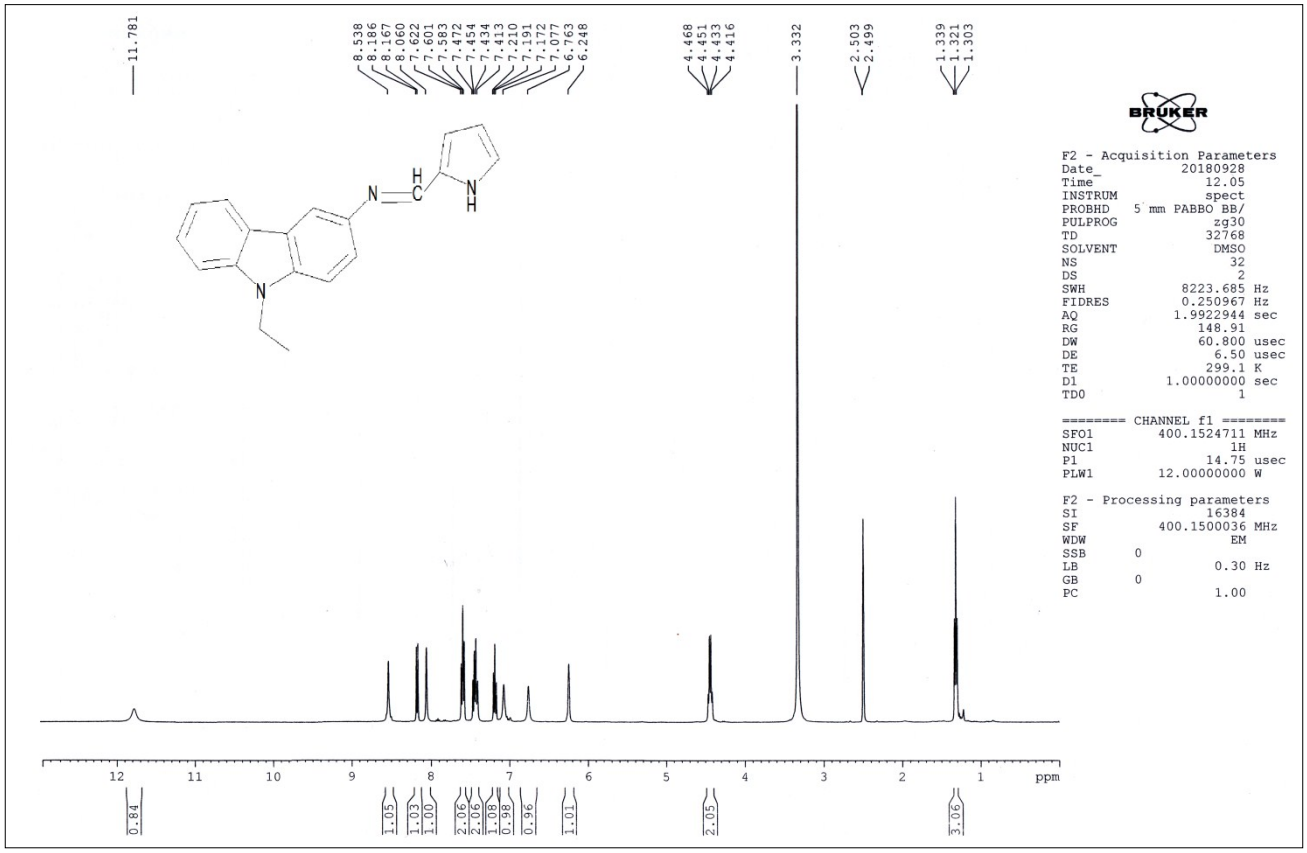

Figure S1.^{1}H NMR of **CPC** in DMSO-d_6 (400 MHz).

^{13}C NMR of CPC in DMSO-d_6:

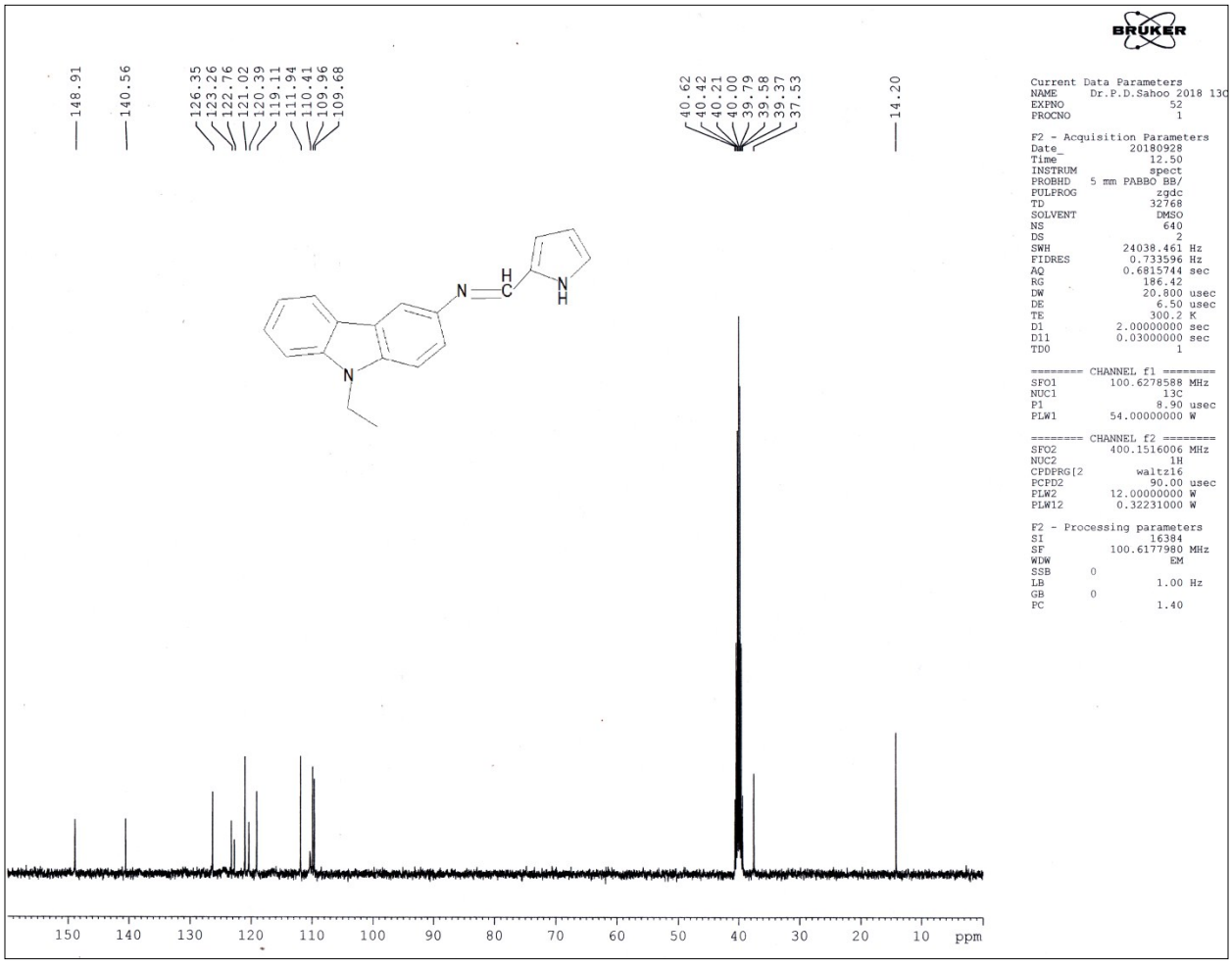

Figure S2.^{13}C NMR of **CPC** in DMSO-d_6 (400 MHz).

2. Mass spectrum of CPC:

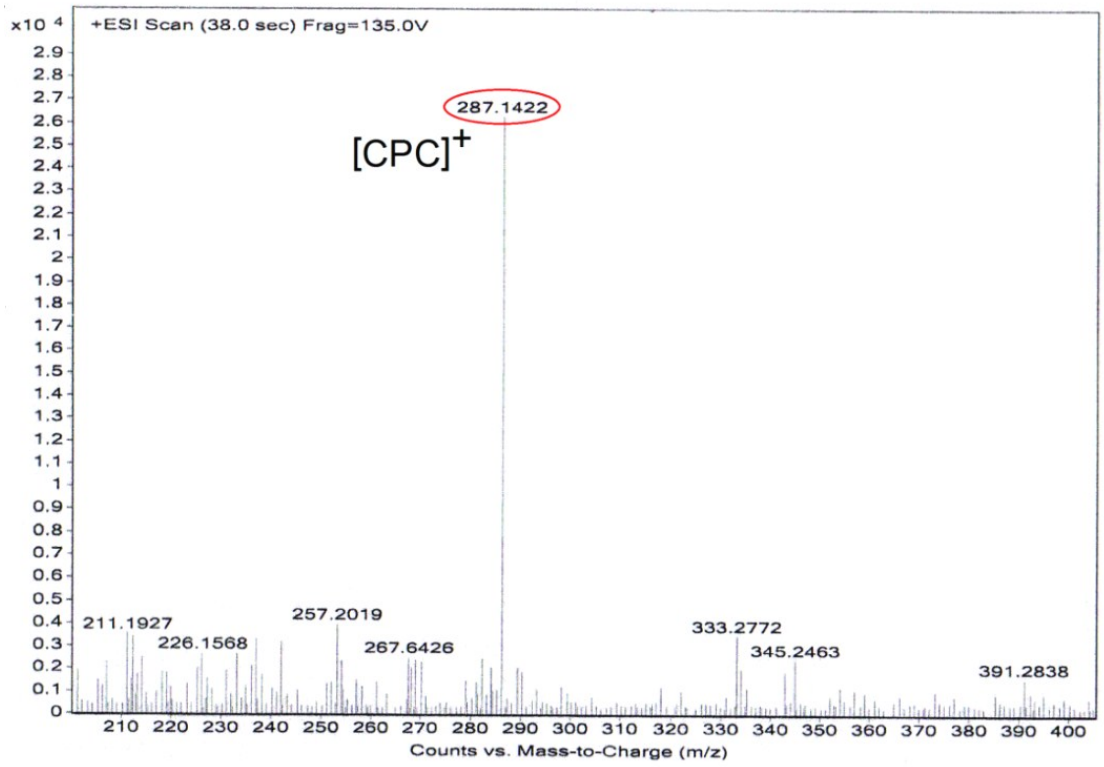

Figure S3. MALDI-TOF MS of **CPC**.

3. **UV-vis spectral studies.**

A stock solution of **CPC** (20 μM) was prepared in the solvent acetonitrile. Cd^{2+} solution (from cadmium perchlorate salt) and DCNP solution of various concentrations were prepared in buffered aqueous medium (pH 7.0, 10 mM phosphate buffer). During the titration of **CPC** with DCNP, each time a 20 μM solution of **CPC** was filled in a quartz optical cell of 1 cm optical path length and DCNP stock solution was added into the quartz optical cell gradually by using a micropipette. The very same method was acquired at the time of titration between **CPC** and Cd^{2+}. Spectral data were recorded at 2-3 min after the addition of Cd^{2+} or DCNP.

4. Evaluation of the Association constants for the formation of CPC-1 by UV-Vis method:

The substrate binding interaction was calculated according to the Benesi-Hildebrand equation.

$$\frac{A_0}{A - A_0} = \left(\frac{\varepsilon_0}{\varepsilon_0 - \varepsilon}\right)^2 \left(\frac{1}{K_B[Substrate]^2} + 1\right)$$

Here A_o is the absorbance of receptor in the absence of guest, A is the absorbance recorded in the presence of added guest, ε_0 and ε are the corresponding molar absorption co-efficient and K_B represents the substrate binding interaction with guest. The association constant (K_a) of was determined from the equation:

K_a = intercept/slope. From the linear fit graph we get, $K_a = 44.9 \times 10^5\ M^{-1}$ for **DCNP**.

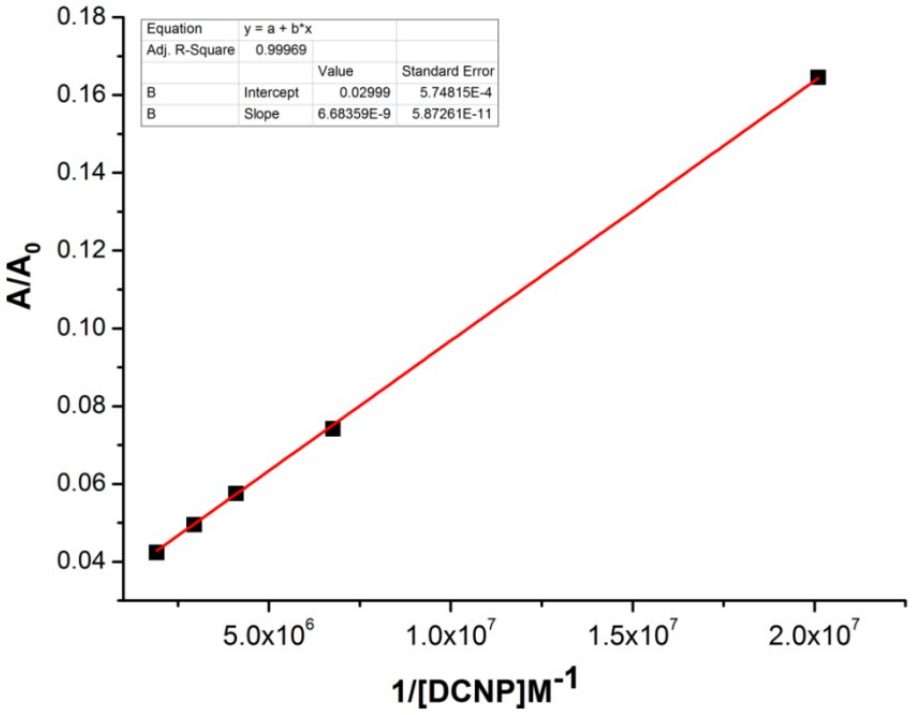

Figure S4. Linear regression analysis (1/[G]vs A/A_0) for the calculation of association constant values of DCNP by UV- titration method.

5. Calculation of limit of detection (LOD) of CPC with DCNP:

The limit of detection (LOD) of **CPC** for sensing **DCNP** was determined from the following equation:

$$LOD = K \times SD/S$$

Where K = 2 or 3 (we take 3 in this case); SD is the standard deviation of the blank receptor solution; S is the slope of the calibration curve.

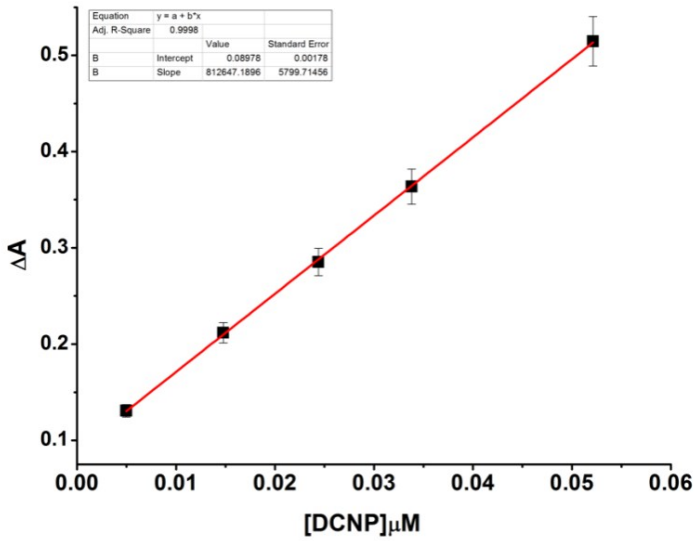

Figure S5. Linear fit curve of **CPC** with respect to DCNP concentration. Standard deviations are given by error bars where, n=3.

From the linear fit graph of **DCNP** (a), we get slope = 8.12×10^5, and SD value is 0.0021.Thus using the above formula we get the Limit of Detection = 7.75×10^{-9} M or 7.75 nM. Therefore, **CPC** can colorimetrically detect **DCNP** up to this very lower concentration.

6. Job's plot for determining the stoichiometry of binding by UV-Vis method:

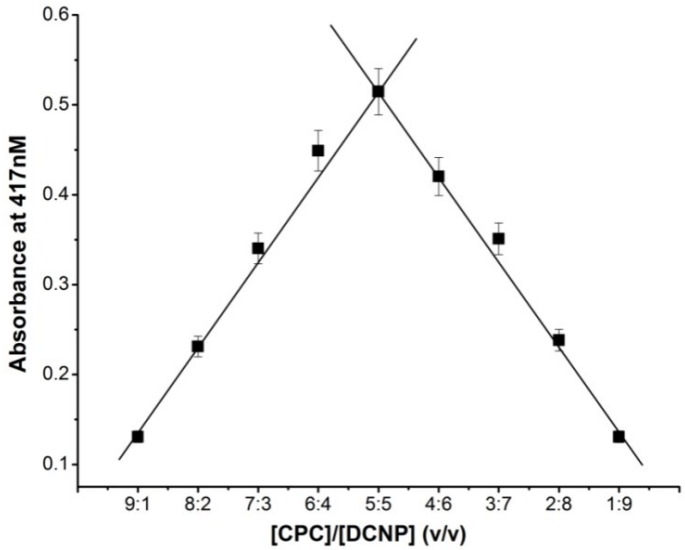

Figure S6. Job's plot of **CPC** with DCNP in acetonitrile-water (1:6, v/v), neutral pH, ([**CPC**] /[DCNP] = 1×10^{-5} M) by UV-Vis method, which indicate 1:1 stoichiometry for **CPC** with DCNP. Standard deviations are given by error bars where, n=3.

7. pH titration of CPC and CPC-1 at varying pH concentrations:

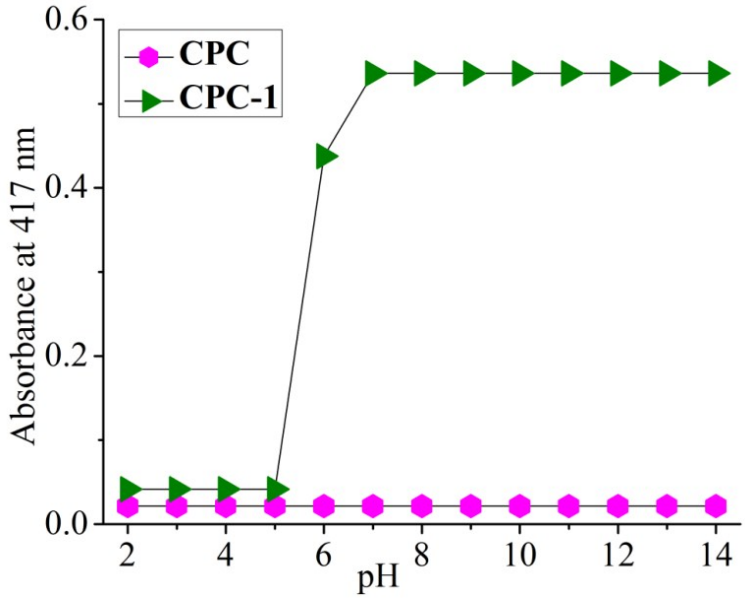

Figure S7. Dependence of the probe **CPC** and the product **CPC-1** on the pH of the solution.

8. Time dependent absorbance changes of CPC upon gradual addition of DCNP:

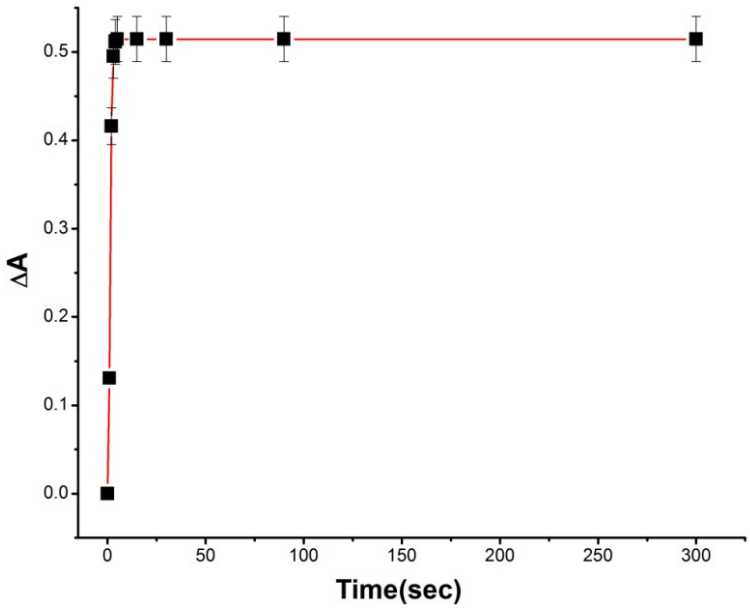

Figure S8. Absorbance intensity plot of **CPC-1** as a function of time in CH_3CN/H_2O (1:6 v/v, pH 7.0, 10 mM phosphate buffer). Standard deviations are given by error bars where, n=3.

9. Fluorescence spectral studies:

A stock solution of **CPC** (20 μM) was prepared in the solvent acetonitrile. Cd^{2+} solution (from cadmium perchlorate salt) and DCNP solution of various concentrations were prepared in buffered aqueous medium (pH 7.0, 10 mM phosphate buffer). During the titration of **CPC** with DCNP, each time a 20 μM solution of **CPC** was filled in a quartz optical cell of 1 cm optical path length and DCNP stock solution was added into the quartz optical cell gradually by using a micropipette. Spectral data were recorded at 2-3 min after the addition of Cd^{2+}. For all fluorescence measurements, excitations were provided at 350 nm, and emissions were collected between 350 to 600 nm.

10. Evaluation of the Association constants for the formation of CPC-Cd^{2+} by fluorescence method.

Binding constant of the **CPC-Cd^{2+}** complex was calculated through emission method by using the following equation.

$$1/ (I - I_0) = 1/K(I_{max} - I_0) [G] + 1/(I_{max} - I_0) \quad (3)$$

where I_0, I_{max}, and I represent the emission intensity of CPC, the maximum emission intensity observed in the presence of added Cd^{2+} at 435 nm (λ_{ex}= 380 nm), and the emission intensity at a certain concentration of the Cd^{2+} respectively. [G] is the concentration of the Cd^{2+} solution added. The association constant (K_a) of was determined from the equation:

K_a = intercept/slope. From the linear fit graph we get, $K_a = 2.83 \times 10^4$ for Cd^{2+}.

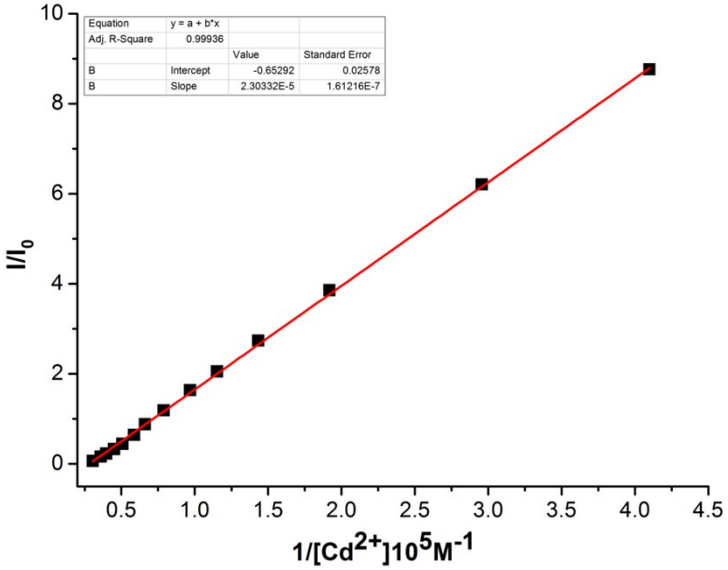

Figure S9. Linear regression analysis (1/[G] vs 1/ΔI) for the calculation of association constant values of Cd^{2+} by Fluorescence titration method.

11. Calculation of limit of detection (LOD) of CPC with Cd^{2+}:

The limit of detection (LOD) of CPC for sensing Cd^{2+} was determined from the following equation:

$$LOD = K \times SD/S$$

Where K = 2 or 3 (we take 3 in this case); SD is the standard deviation of the blank receptor solution; S is the slope of the calibration curve.

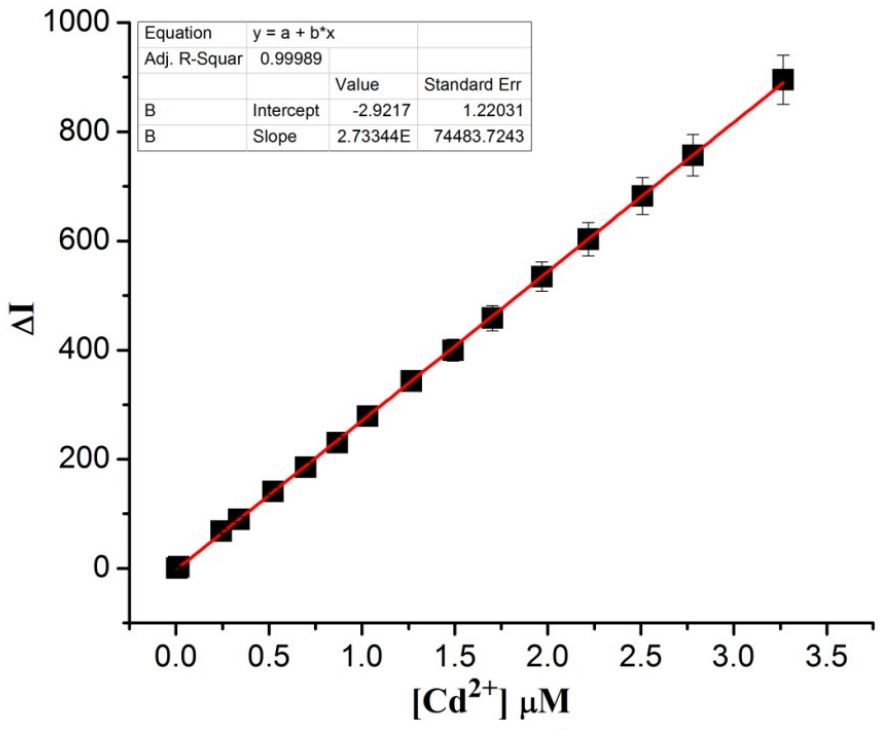

Figure S10. Linear fit curve of **CPC** with respect to Cd^{2+}concentration.

From the linear fit graph of Cd^{2+} we get slope = 2.73×10^{7} and SD value is 2.49. Thus using the above formula we get the Limit of Detection = 0.27×10^{-6} M or 0.27 μM. Therefore **CPC** can detect Cd^{2+} up to this very lower concentration by fluorescence techniques. An average of three replicate measurements with standard deviation has been taken in each case.

12. Job's plot for determining the stoichiometry of binding by fluorescence method:

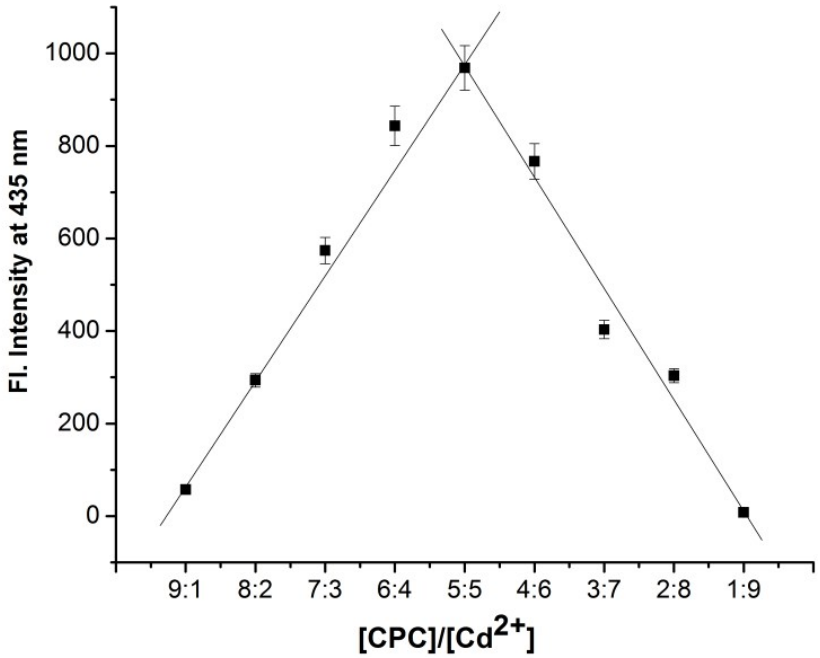

Figure S11. Job's plot of **CPC** with Cd^{2+} in acetonitrile-water (1:6, v/v), ([**CPC**] / [Cd^{2+}] = 1 × 10^{-5} M) by fluorescence method, which indicate 1:1 stoichiometry for **CPC** with Cd^{2+}. An average of three replicate measurements with standard deviation was taken for each value.

13. Time dependent fluorescence changes of CPC upon gradual addition ofCd^{2+}:

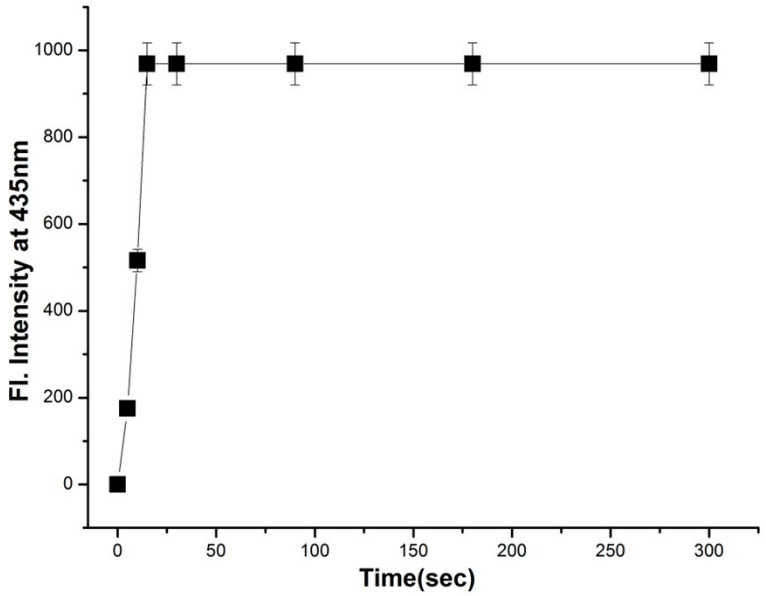

Figure S12. Fluorescence intensity plot of **CPC**-Cd^{2+} complex as a function of time in CH_3CN/H_2O (1:6, v/v, pH 7.0, 10 mM phosphate buffer). An average of three replicate measurements with standard deviation was taken.

14. pH dependence of probe CPC and CPC-Cd^{2+} complex:

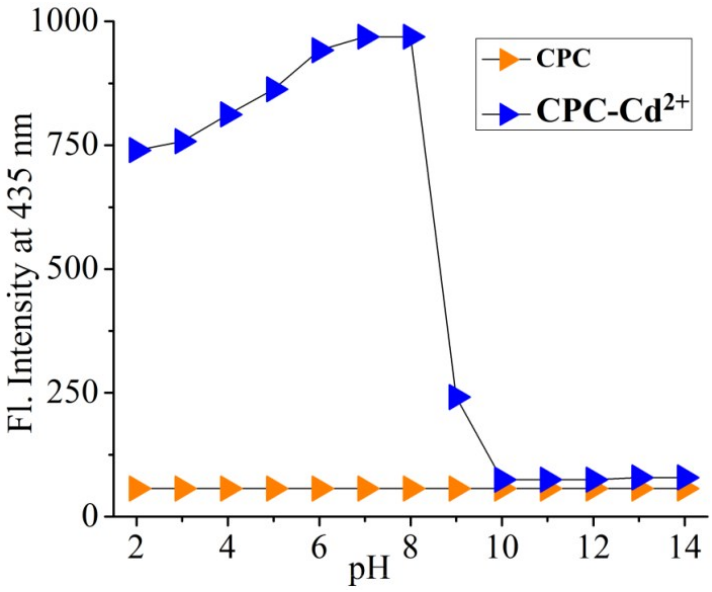

Figure S13. Dependence of the probe **CPC** and the complex **CPC-Cd^{2+}** on the pH of the solution.

15. HMQC spectra:

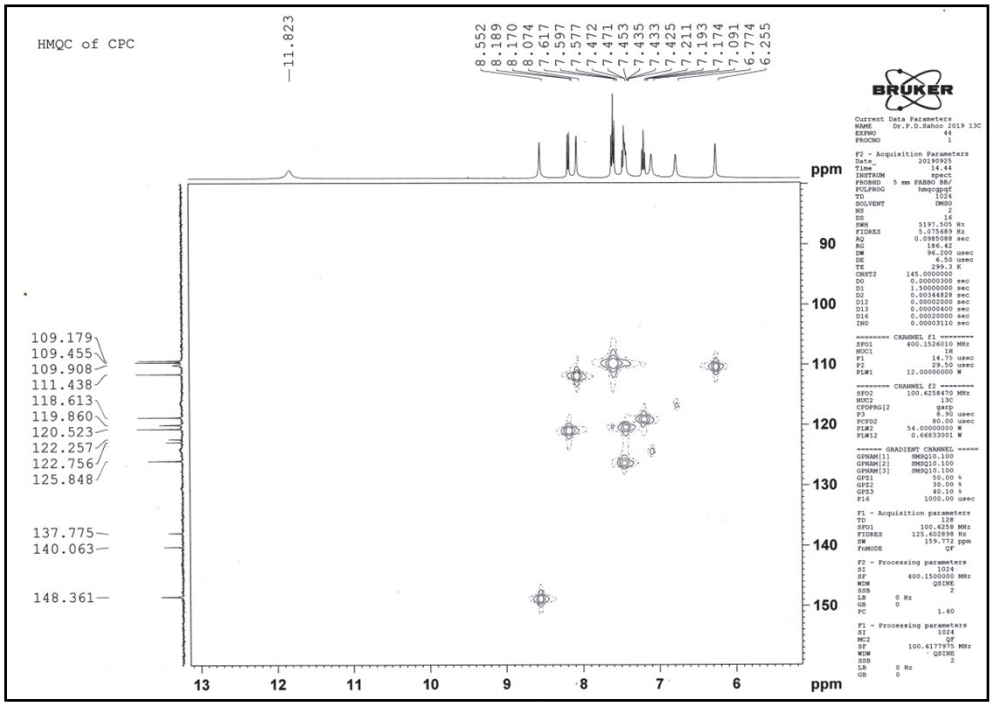

Figure S14. HMQC spectra [400 MHz] of **CPC** in DMSO-d_6 at 25^0C.

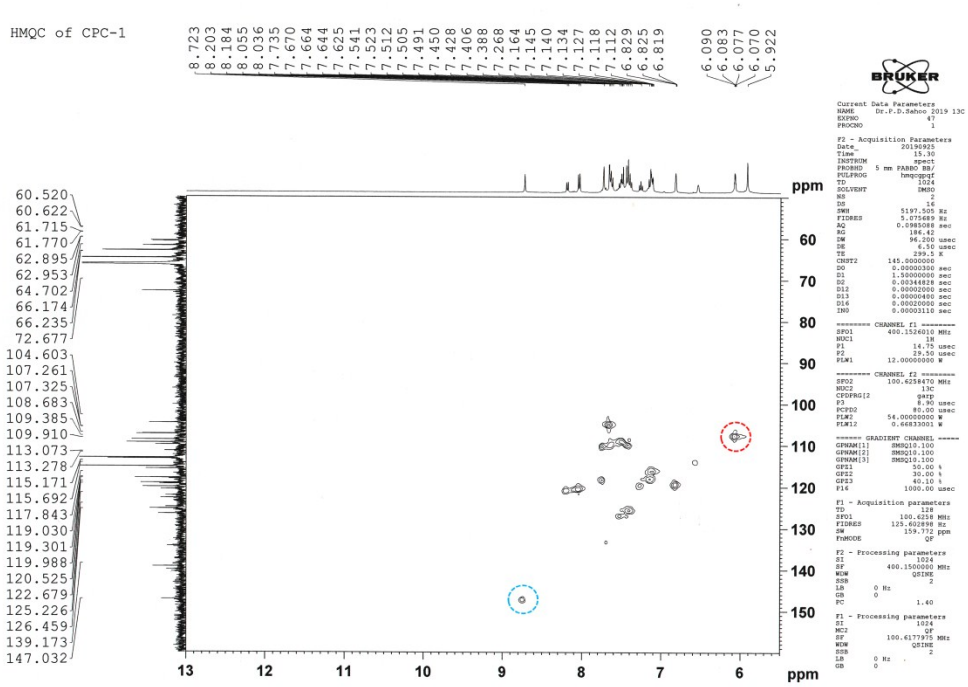

Figure S15. HMQC spectra [400 MHz] of **CPC-1** in DMSO-d_6 at 25^0c

16. Mass spectroscopic titrations:

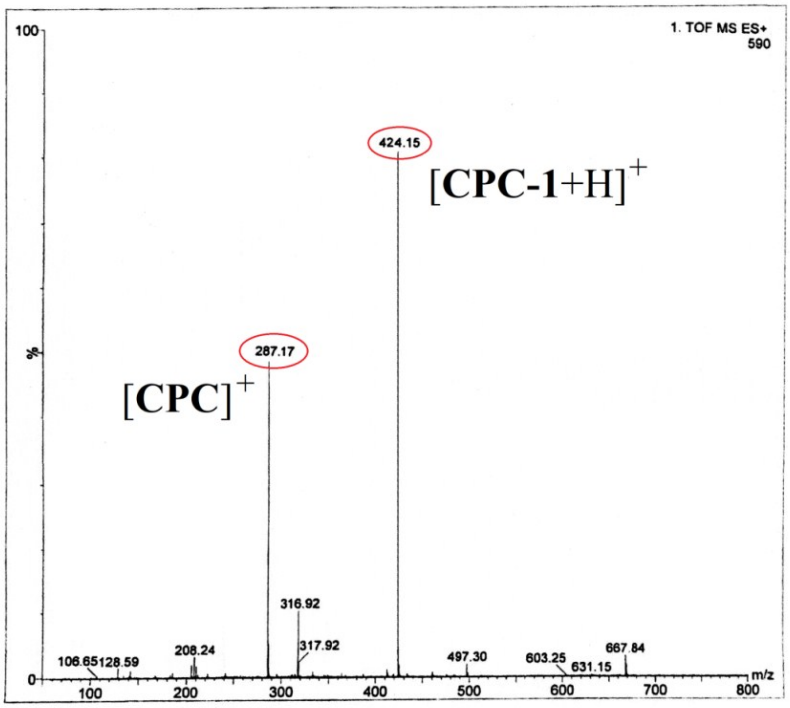

Figure S16. Partial HRMS spectra of the **CPC**-DCNP mixture taken after four hours of addition of DCNP to the **CPC** in acetonitrile.

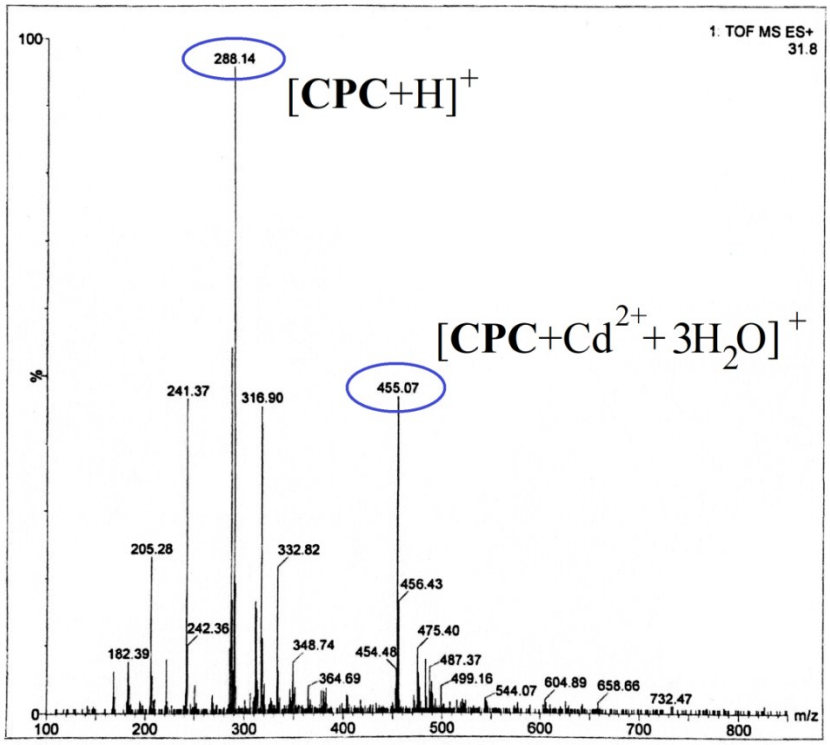

Figure S17. Partial HRMS spectra of the **CPC**-Cd^{2+} mixture taken after two hours of addition of Cd^{2+} to the **CPC** in acetonitrile.

17. Details of energy calculations using Density Functional Theory (DFT):

Top view of energy optimized geometry:

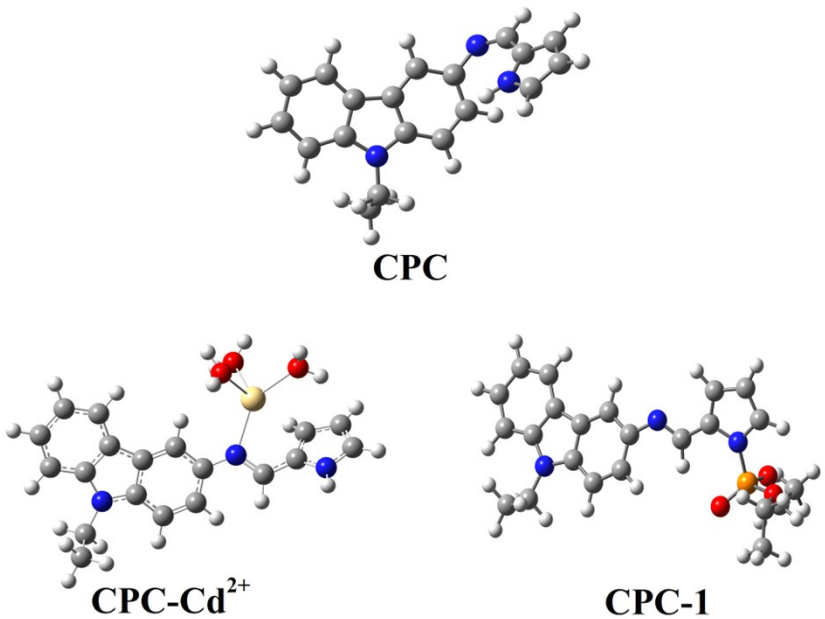

Figure S18. Energy optimized geometries of **CPC**, **CPC-1** and **CPC-Cd^{2+}** complex obtained at the B3LYP/6-311G(d,p)/LANL2DZ levels of theory with CPCM solvation (H_2O).

Table S2. Details of the geometry optimization in Gaussian 09 program.

Details	CPC-*cis*	CPC-*trans*	CPC-1	CPC-Cd^{2+}	DCNP
Calculation method	RB3LYP	RB3LYP	RB3LYP	RB3LYP	RB3LYP
Basis set	6-311G**	6-311G**	6-311G**	6-311G**	6-311G**
E(RB3LYP) (a.u.)	-898.748	-898.753	-1623.834	-1175.692	-818.538
Charge, Multiplicity	0, 1	0, 1	0, 1	2, 1	0, 1
Solvent (CPCM)	Water	Water	Water	Water	Water

Table S3. Selected electronic excitation energies (eV), oscillator strengths (f), main configurations of the low-lying excited states of all the molecules and complexes. The data were calculated by TDDFT//B3LYP/6-311G (d,p) based on the optimized ground state geometries.

Molecules	Electronic Transition	Excitation Energy[a]	f[b]	Composition[c](%)
CPC	$S_0 \rightarrow S_1$	3.38 eV at 366.84 nm	0.8424	H→ L (69.33 %)
	$S_0 \rightarrow S_4$	4.29 eVat 288.91nm	0.4564	H-1→ L+1 (55 %)
CPC-Cd^{2+}	$S_0 \rightarrow S_2$	3.07 eV at 403.61 nm	0.5608	H → L+1 (64.5 %) H-1 → L (26.5 %)
	$S_0 \rightarrow S_8$	4.30 eV at 287.96 nm	0.1595	H-2 → L+1 (53 %) H-4 → L (42.4 %)

CPC-1	$S_0 \rightarrow S_1$	3.21 eV at 390.12 nm	0.8338	H→ L (69.7 %)
	$S_0 \rightarrow S_4$	4.23 eV at 292.84 nm	0.3988	H-3 → L (47.8 %)

Table S4. Energies of the highest occupied molecular orbital (HOMO) and lowest unoccupied molecular orbital (LUMO).

Species	**E_{HOMO} (a.u)**	**E_{LUMO} (a.u)**	**ΔE(a.u)**	**ΔE(eV)**	**ΔE(kcal/mol)**
CPC	-0.19666	-0.05505	0.14161	3.85	88.86
CPC-Cd^{2+}	-0.2053	-0.07384	0.13146	3.57	82.38
CPC-1	-0.19915	-0.06495	0.1342	3.65	84.20

18. Proposed Mechanism for the formation of CPC-1:

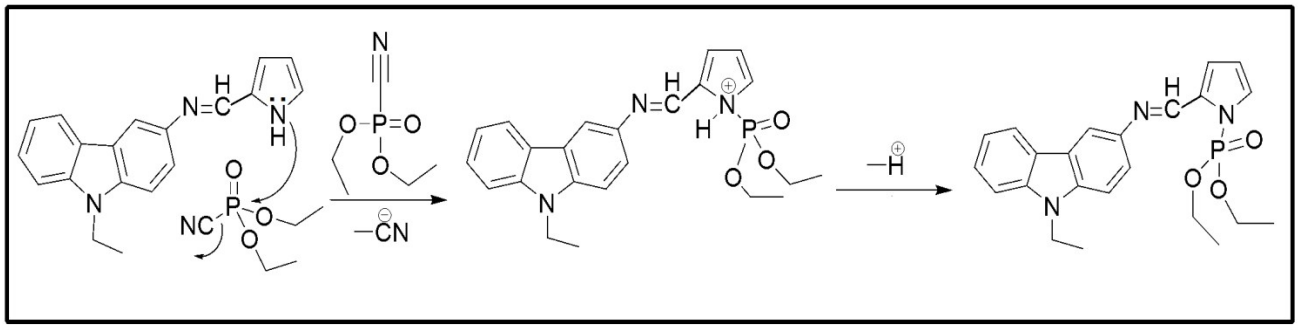

Scheme S1. Proposed mechanism for the formation of **CPC-1** from **CPC** upon addition of 1 equivalent of DCNP.

19. Quantification of DCNP in water samples by UV-Vis method:

Concentration vs. absorbance intensity graph for quantification of DCNP in pond and sea water samples:

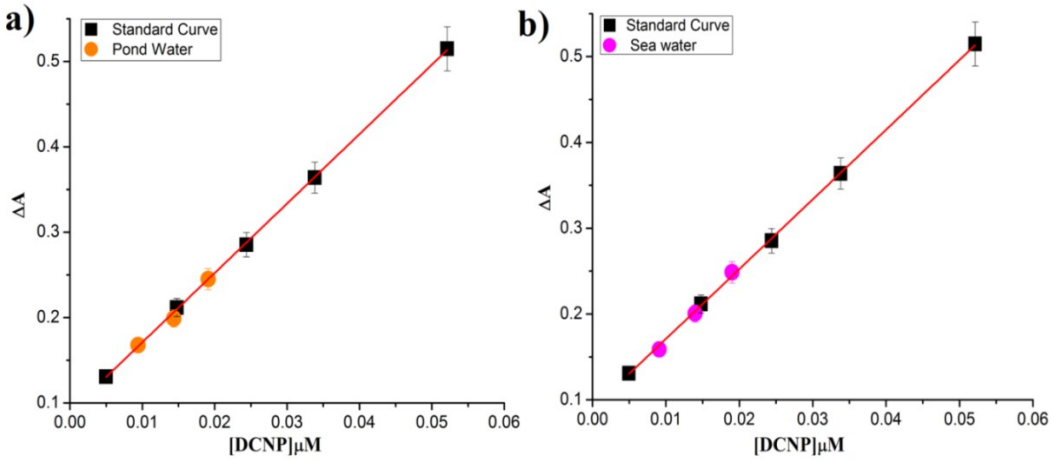

Figure S19. (a) Estimation of concentration of DCNP added in pond water samples following the standard curve. (b) Estimation of concentration of DCNP added in sea water samples following the standard curve. Standard deviations are given by error bars where, n=3.

20. Quantification of Cd^{2+} in water samples by fluorescence method:

Concentration vs. fluorescence intensity graph for quantification of Cd^{2+} in pond and sea water samples:

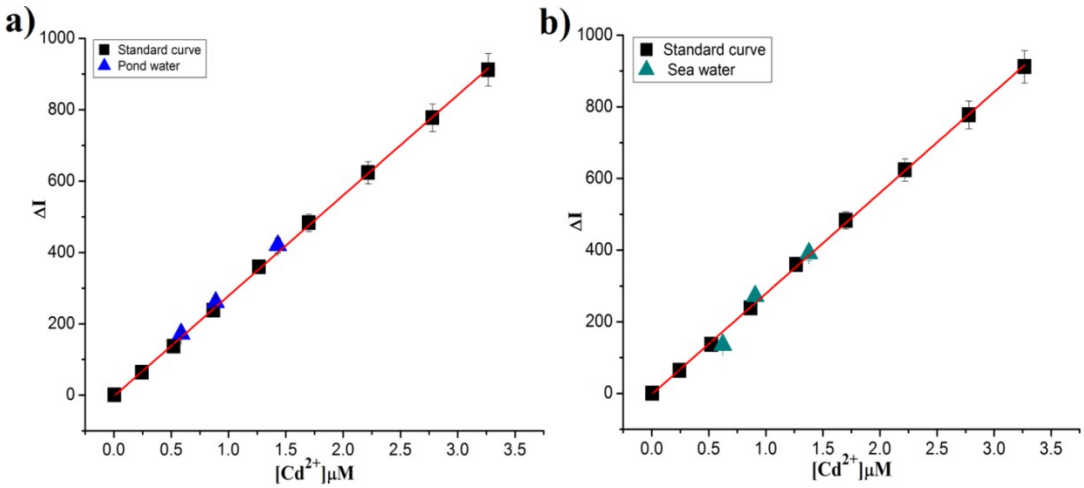

Figure S20. (a) Estimation of concentration of Cd^{2+} added in pond water samples following the standard curve. (b) Estimation of concentration of Cd^{2+} added in sea water samples following the standard curve. Standard deviations are given by error bars where, n=3.